Int. J. Solids Structures, 1974, Vol. 10, pp. 883–902. Pergamon Press. Printed in Gt. Britain.

IMPERFECTION SENSITIVITY OF AXIALLY COMPRESSED STRINGER REINFORCED CYLINDRICAL SANDWICH PANELS

NELSON R. BAULD, JR.
Clemson University, Clemson, South Carolina 29631, U.S.A.

(*Received* 14 *September* 1973)

Abstract—This paper presents some numerical results of the effects of several nondimensional parameters on the buckling and initial post buckling behaviors of shallow sandwich panels under axial compression. Results are presented that show these effects due to transverse shearing resistance of the core material, different face-sheet thicknesses, and different core thicknesses. Further effects on the buckling and initial postbuckling behaviors of sandwich panels are presented due to the torsional resistance of longitudinal edge stiffeners.

The results show that the range of flatness parameter, δ/d, for which sandwich panels remain imperfection-insensitive increases with increases in transverse shearing resistance of the core material and with larger core thicknesses. These results also indicate that this range of δ/d is smallest when the face-sheet thicknesses are equal. Finally, as in the case of homogeneous panels, torsional resistance of the longitudinal edge stiffeners has the effect of making the sandwich panel less imperfection-sensitive.

NOMENCLATURE

a, b	initial postbuckling coefficients defined in equation (60)
B_1, B_2	extensional stiffnesses of the outer and inner face-sheets defined in equation (5)
c	core thickness
$2d$	projection of the circumferential distance on the reference surface of the composite panel onto its base plane
D_1, D_2	flexural stiffnesses of the outer and inner face-sheets
e, e_0	average end-shortening parameter and its value for the prebuckled state at the bifurcation point
E_1, E_2	Young's moduli for the outer and inner face-sheets
G_{xz}, G_{yz}	transverse shearing moduli for the core material
$g_1(\eta), g_2(\eta)$	functions defined by equations (40) and (41)
$h_1(\eta), h_2(\eta)$	functions defined by equations (42) and (43)
h	distance between reference surfaces of the face-sheets
JG	torsional stiffness of the longitudinal stiffeners
K	ratio of the panel stiffness after buckling to its stiffness prior to buckling. Defined in equation (64)
k	nondimensional parameter $(\sqrt{3(1-\nu^2)})$
M_x^i, M_y^i, M_{xy}^i	bending and twisting moments associated with the ith face-sheet
N_x^i, N_y^i, N_{xy}^i	normal and shearing stress-resultants associated with the ith face-sheet
Q_x^i, Q_y^i	transverse shearing stress-resultants associated with the ith face-sheet
q_0	nondimensional parameter $(\sqrt{2kR/t^*})$
R	radius of curvature of the reference surface for the composite panel
s	relative stiffness parameter defined in equation (65)
S_0, S	slopes of the load-deflection curve immediately before and after buckling
t^*	weighted thickness of the panel
t_1, t_2	thicknesses of the outer and inner face-sheets
$U, V, W; u, v, w$	physical axial, circumferential, and normal displacements of points on the reference surface; dimensionless counterparts
x, y	physical axial and circumferential coordinates on the reference surface

$\bar{\alpha}, \bar{\beta}; \alpha, \beta$	physical shear angles for the core material in the x and y directions; dimensionless counterparts
γ_1, γ_2	nondimensional parameters associated with the torsional resistance of the longitudinal stiffeners defined in equation (26)
δ	rise of panel above its base plane
Δ	nondimensional parameter defined in equation (63)
ε	infinitesimal scalar parameter defined in equation (60)
$\bar{\varepsilon}_x$	physical axial strain associated with the reference surface of the composite panel
ξ, η	nondimensional axial and circumferential coordinates
$\bar{\eta}$	value of η at the longitudinal stiffener
$\Psi, \chi, \vartheta \tau$	postbuckling functions defined in equation (44)
ρ, μ	postbuckling functions defined in equation (44)
θ, ω	postbuckling functions defined in equation (44)
λ	nondimensional parameter defined in equation (15)
λ^*	ratio of the length of the buckled wave in circumferential direction to the half length of the buckled wave in the axial direction
ν	Poisson ratio's for the face-sheets
σ, σ_c	nondimensional load parameter and its value at the bifurcation point
σ_c^*	modified critical value of nondimensional load parameter ($\sigma_c^* = \sigma_c / R/t^*$)
$\Lambda_1, \Lambda_2, \Lambda_3, \Lambda_4$	nondimensional reactions of the core material on the face-sheets defined in equations (1–4)
Φ, ϕ	physical and nondimensional airy stress functions.

INTRODUCTION

The aerospace industry has been interested in sandwich type constructions since the end of World War II because of the relatively high strength-weight ratios that structural components made in this composite manner exhibit. Conceptual models[1, 2] for sandwich panels have appeared in the literature that view the composite structural element as consisting of two distinct, thin, isotropic, face-sheets that are separated by a suitable lightweight core material that is, itself, assumed to be either an isotropic or an orthotropic continuum. More recently, additional improvements in the strength–weight ratios of composites of varying geometric configurations have been realized through the use of fiber-reinforced, layered shells as face-sheets. This improvement in the strength–weight ratio of the composite structural element arises because of the increased strength–weight ratio of the individual fibers and the capability of arranging the fiber orientations so as to obtain a minimum weight for the composite structural element without compromising its load carrying capacity.

Considerable work has been done relative to obtaining information concerning the buckling and initial post-buckling behaviors of fiber-reinforced, layered, complete cylindrical shells under axial and lateral pressure[3–5]. Even more work has been done regarding these behaviors for isotropic shells of various geometries and loading conditions[6]. These works, however, with the exception of those of[7], have not encompassed the sandwich concept as detailed in the opening paragraph.

The present investigation is confined to the study of the buckling and initial post-buckling behavior of edge-stiffened, circular cylindrical, composite panels with isotropic face-sheets under uniform axial compression. The composite panel consists of two isotropic face-sheets that are separated by an orthotropic core material. The face-sheets may have unequal thicknesses and be of different materials, while the core material is considered to be capable of transmitting only transverse shearing forces. Thus, the in-plane resistance of the core material is assumed to be negligible in comparison to the in-plane resistances of the face-sheets. Furthermore, transverse normal deformations in the core material are also ignored.

The straight edges of the sandwich panel are assumed to be reinforced by stiffeners that are constrained to stay in the undeformed reference surface of the panel. Therefore, it is assumed that the flexural stiffness of the longitudinal stiffeners relative to axes normal to the straight edges of the panel is infinite. The flexural stiffness of the stiffeners relative to axes normal to the reference surface of the composite panel is considered to be negligible; thus, the circumferential displacements of the straight edges of the panel are unconstrained by the stiffeners. Finally, the stiffeners are assumed to twist freely about their entire length. The boundary conditions used in this study incorporate the conditions used by Koiter[8] in his study of the buckling and initial post-buckling behaviors of longitudinally reinforced, narrow, homogeneous panels under axial compression which are identical to those used by Stephens[9] in extending Koiter's analysis to include the torsional resistance of longitudinal stiffeners.

The theoretical basis for the present study is essentially a perturbation technique proposed by Koiter[10] and that was transcribed by Budiansky[11] into a form more suitable for application to thin shell type structures whose prebuckling behavior is linear.

MATHEMATICAL MODEL

The field equations governing the moderately large deflections of circular, cylindrical, sandwich panels derived by Fulton[1] can be expressed in the following form:

$$\nabla^4 w + \phi_{,\xi\xi} - 2k(\phi_{,\eta\eta} w_{,\xi\xi} - 2\phi_{,\xi\eta} w_{,\xi\eta} + \phi_{,\xi\xi} w_{,\eta\eta}) - \Lambda_1(\alpha + w_{,\xi})_{,\xi} - \Lambda_2(\beta + w_{,\eta})_{,\eta} = 0, \quad (1)$$

$$\nabla^4 \phi - w_{,\xi\xi} - 2k(w_{,\xi\eta}^2 - w_{,\xi\xi} w_{,\eta\eta}) = 0, \quad (2)$$

$$\frac{1-\nu}{2}\nabla^2\alpha + \frac{1+\nu}{2}(\alpha_{,\xi} + \beta_{,\eta})_{,\eta} - \Lambda_3(\alpha + w_{,\xi}) = 0, \quad (3)$$

$$\frac{1-\nu}{2}\nabla^2\beta + \frac{1+\nu}{2}(\alpha_{,\xi} + \beta_{,\eta})_{,\eta} - \Lambda_4(\beta + w_{,\eta}) = 0. \quad (4)$$

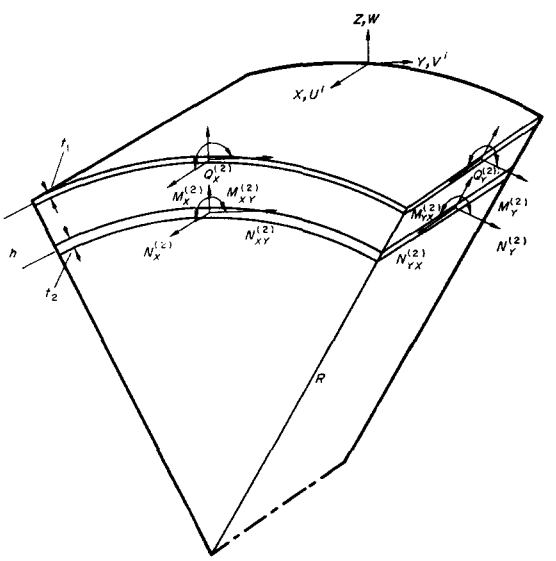

Fig. 1. Circular cylindrical sandwich panel.

The signs of some of the terms in these equations differ from those presented by Fulton; however, they are fully equivalent. The differences arise because of the sign convention on w and the definitions of the quantities α and β.

The nondimensional quantities appearing in equations (1–4) are related to the corresponding physical quantities through the relations

$$\xi = \frac{q_0}{R}x,\ \eta = \frac{q_0}{R}y,\ q_0 = (2k^R/_t{}^*)^{1/2},\ k = [3(1-\nu^2)]^{1/2},$$

$$(t^*)^2 = \frac{E_1t_1^3 + E_2t_2^3}{E_1t_1 + E_2t_2},\ w = \frac{w}{t^*},\ \phi = \frac{2k}{(E_1t_1 + E_2t_2)(t^*)^2}\Phi,$$

$$\alpha = \frac{R}{t^*}\frac{\bar{\alpha}}{q_0},\ \beta = \frac{R}{t^*}\frac{\bar{\beta}}{q_0},\ \Lambda_1 = \frac{G_{xz}h^2q_0^2}{c[E_1t_1 + E_2t_2]},\ \Lambda_2 = \frac{G_{yz}h^2q_0^2}{c[E_1t_1 + E_2t_2]},$$

$$\Lambda_3 = \frac{G_{xz}(B_1 + B_2)}{cB_1B_2}\left(\frac{R}{q_0}\right)^2,\ \Lambda_4 = \frac{G_{yz}(B_1 + B_2)}{cB_1B_2}\left(\frac{R}{q_0}\right)^2,\ \sigma = \frac{N_x}{t^*}\frac{Rk}{(E_1t_1 + E_2t_2]}.$$

In the foregoing expressions R is the radius of the composite panel, t_1 and t_2 denote face-sheet thicknesses, and c signifies the core thickness. Young's moduli for the face-sheets are denoted by E_1 and E_2, the transverse shearing moduli for the core material by G_{xz} and G_{yz}, and Poisson's ratio by ν. The quantities w, ϕ, α, β are the nondimensional transverse deflection, airy stress function, and core shearing angles in the axial and circumferential directions, respectively; and W, Φ, $\bar{\alpha}$, $\bar{\beta}$ are the corresponding physical quantities. The in-plane stiffnesses of the face-sheets are defined by the relations

$$B_i = \frac{E_it_i}{1-\nu^2}\ (i = 1,2), \tag{5}$$

where $i = 2$ denotes the face-sheet nearest the center of curvature and $i = 1$ denotes the other. The distance between the middle surfaces of the two face-sheets is signified by h, and ξ, η are the nondimensional axial and circumferential coordinates corresponding to the physical coordinates x, y. Finally, the Laplacian operator in equations (1–4) is given by

$$\nabla(\ \ ) \equiv (\ \ )_{,\xi\xi} + (\ \ )_{,\eta\eta}. \tag{6}$$

Average end-shortening parameter

In order to compare the stiffness of the composite panel in its prebuckled and initial post-buckled states an average end-shortening parameter is defined through the relation

$$e = \frac{1}{2d}\int_A \bar{\varepsilon}_x\,dx\,dy \tag{7}$$

where $\bar{\varepsilon}_x$ is the physical axial strain associated with the reference surface of the composite panel and $2d$ is the projection of the circumferential length of this reference surface onto the base plane of the panel. For a membrane prebuckled state, equation (7) reduces to the nondimensional form

$$e_0 = \frac{(t^*)^2\sigma_c}{4dk^2}\int_A d\xi\,d\eta. \tag{8}$$

Here σ_c is the value of the nondimensional load parameter at the bifurcation point. Defining the prebuckling stiffness of the composite panel by S_0 one obtains from equation (8)

$$\frac{1}{S_0} = \left.\frac{\mathrm{d}e_0}{\mathrm{d}\sigma}\right|_{\sigma=\sigma_c} = \frac{(t^*)^2}{4dk^2}\int_A \mathrm{d}\xi\,\mathrm{d}\eta. \tag{9}$$

Buckling equations

To study the buckling behavior of the cylindrical sandwich panel a solution of equations (1–4) is sought in the form

$$\begin{Bmatrix} w \\ \phi \\ \alpha \\ \beta \end{Bmatrix} = \sigma \begin{Bmatrix} w_0 \\ \phi_0 \\ \alpha_0 \\ \beta_0 \end{Bmatrix} + \varepsilon \begin{Bmatrix} w_1 \\ \phi_1 \\ \alpha_1 \\ \beta_1 \end{Bmatrix} + 0(\varepsilon^2). \tag{10}$$

Here ε is an infinitesimal scalar parameter and σ is a nondimensional load parameter. Substituting equations (10) into equations (1–4), recalling that the prebuckled state is assumed to be a membrane state ($\phi_0 = -\eta^2/2k$, $w_0 = \text{constant}$, $\alpha_0 = \alpha_0 = 0$), and linearizing with respect to ε, one obtains the system of differential equations

$$\nabla^4 w_1 + \phi_{1,\xi\xi} + 2\sigma w_{1,\xi\xi} - \Lambda_1(\alpha_1 + w_{1,\xi})_{,\xi} - \Lambda_2(\beta_1 + w_{1,\eta})_{,\eta} = 0, \tag{11}$$

$$\nabla^4 \phi_1 - w_{1,\xi\xi} = 0, \tag{12}$$

$$\frac{1-\nu}{2}\nabla^2\alpha_1 + \frac{1+\nu}{2}(\alpha_{1,\xi} + \beta_{1,\eta})_{,\xi} - \Lambda_3(\alpha_1 + w_{1,\xi}) = 0, \tag{13}$$

$$\frac{1-\nu}{2}\nabla^2\beta_1 + \frac{1+\nu}{2}(\alpha_{1,\xi} + \beta_{1,\eta})_{,\eta} - \Lambda_4(\beta_1 + w_{1,\eta}) = 0. \tag{14}$$

Since the panel is assumed to be long compared to its width the boundary conditions at the ends will not effect the buckling load; consequently, a solution to equations (11–14) is assumed in the form

$$\begin{aligned} w_1(\xi,\eta) &= w_1(\eta)\cos\frac{\pi\xi}{\lambda}, \\ \phi_1(\xi,\eta) &= \phi_1(\eta)\cos\frac{\pi\xi}{\lambda}, \\ \alpha_1(\xi,\eta) &= \alpha_1(\eta)\sin\frac{\pi\xi}{\lambda}, \\ \beta_1(\xi,\eta) &= \beta_1(\eta)\cos\frac{\pi\xi}{\lambda}. \end{aligned} \tag{15}$$

The ξ dependence of equations (11–14) is eliminated by means of equations (15). One obtains, in this manner, a set of homogeneous, ordinary differential equations:

$$\begin{aligned} w_1^{iv} - \left[\Lambda_2 + 2\left(\frac{\pi}{\lambda}\right)^2\right]w_1'' + \left[\left(\frac{\pi}{\lambda}\right)^4 - 2\sigma\left(\frac{\pi}{\lambda}\right)^2 + \Lambda_1\left(\frac{\pi}{\lambda}\right)^2\right]w_1 \\ - \left(\frac{\pi}{\lambda}\right)^2\phi_1 - \Lambda_1\left(\frac{\pi}{\lambda}\right)\alpha_1 - \Lambda_2\beta_1' = 0, \end{aligned} \tag{16}$$

$$\phi_1^{iv} - 2\left(\frac{\pi}{\lambda}\right)^2 \phi_1'' + (\pi/\lambda)^4 \phi_1 + (\pi/\lambda)^2 w_1 = 0, \tag{17}$$

$$\frac{1-\nu}{2}\alpha_1'' - [\Lambda_3 + (\pi/\lambda)^2]\alpha_1 - \frac{1+\nu}{2}\left(\frac{\pi}{\lambda}\right)\beta_1' + \Lambda_3(\pi/\lambda)w_1 = 0, \tag{18}$$

$$\beta_1'' - \left[\Lambda_4 + \frac{1-\nu}{2}\left(\frac{\pi}{\lambda}\right)^2\right]\beta_1 + \frac{1+\nu}{2}\left(\frac{\pi}{\lambda}\right)\alpha_1' - \Lambda_4 w_1' = 0. \tag{19}$$

To obtain suitable boundary conditions to accompany equations (16–19) certain simplifying assumptions are made along the straight edges of the panel. Thus, the edges are assumed to remain straight and the flexural rigidity of the stiffeners about a normal to the reference surface of the panel is neglected. These conditions, together with the evenness of the tangential displacement v about the stiffener, yield the following boundary conditions along the straight edges:

$$w_1(\bar{\eta}) = 0, \tag{20}$$

$$w_1''(\bar{\eta}) + \gamma_1(\pi/\lambda)^2 w'(\bar{\eta}) = 0, \tag{21}$$

$$\phi_1(\bar{\eta}) = 0, \tag{22}$$

$$\phi_1''(\bar{\eta}) = 0, \tag{23}$$

$$\alpha_1'(\bar{\eta}) - (\pi/\lambda)\beta_1(\bar{\eta}) = 0, \tag{24}$$

$$\beta_1'(\bar{\eta}) + \nu(\pi/\lambda)\alpha_1(\bar{\eta}) + \gamma_2\left(\frac{\pi}{\lambda}\right)^2 \beta_1(\bar{\eta}) = 0. \tag{25}$$

Here $\gamma_1 = \dfrac{JG}{D_1 + D_2} q_0/R$ and $\gamma_2 = \dfrac{JG}{h}\dfrac{q_0}{R}\dfrac{B_1 + B_2}{B_1 B_2}$. (26)

The torsional resistance of the longitudinal stringers is denoted by JG and the flexural stiffnesses of the face-sheets by

$$D_i = \frac{E_i t_i^3}{12(1-\nu^2)}. \tag{27}$$

Equations (20–23) are Koiter type boundary conditions similar to those used in[8, 9]. Conditions (24) and (25) stipulate that the bending and twisting moments due to the membrane forces in the face-sheets vanish.

The buckling mode $(w_1, \phi_1, \alpha_1, \beta_1)$ is assumed to be symmetrical so that symmetry considerations at the center of the panel lead to

$$w_1(0) = 0, \tag{28}$$

$$w_1'''(0) = 0, \tag{29}$$

$$\phi_1'(0) = 0, \tag{30}$$

$$\phi_1'''(0) = 0, \tag{31}$$

$$\alpha_1'(0) = 0, \tag{32}$$

$$\beta_1(0) = 0. \tag{33}$$

Equations (16–19) together with the boundary conditions (20–25) and (28–33) constitute a linear eigenvalue problem that determines the critical value of the load parameter σ and the buckling quantities w_1, ϕ_1, α_1, β_1 associated with it. In the foregoing equations, and in all subsequent work, differentiation with respect to η is signified by $(\ )'$. The critical value of the nondimensional load parameter σ corresponds to the minimum value of σ on the set of values associated with λ. The ratio of the length of the buckled mode in the circumferential direction to the length of the buckled mode in the axial direction is given by

$$\lambda^* = \frac{2d}{l} = \frac{2q_0}{\lambda}\frac{d}{R}. \tag{34}$$

Initial post-buckling behavior

To investigate the initial postbuckling behavior of the sandwich panel, the quantities w, ϕ, α, β are expanded in asymptotic series of the infinitesimal scalar parameter ε. Accordingly,

$$\begin{Bmatrix} w \\ \phi \\ \alpha \\ \beta \end{Bmatrix} = \sigma \begin{Bmatrix} w_0 \\ \phi_0 \\ \alpha_0 \\ \beta_0 \end{Bmatrix} + \varepsilon \begin{Bmatrix} w_1 \\ \phi_1 \\ \alpha_1 \\ \beta_1 \end{Bmatrix} + \varepsilon^2 \begin{Bmatrix} w_2 \\ \phi_2 \\ \alpha_2 \\ \beta_2 \end{Bmatrix} + 0(\varepsilon^3) \tag{35}$$

Substituting equation (35) into the general nonlinear equilibrium equations (1–4), observing that at the bifurcation point ω_0, ϕ_0, α_0, β_0 satisfy the equations associated with the prebuckled equilibrium state and w_1, ϕ_1, α_1, β_1 satisfy equations (11–14) associated with the buckling mode, and letting $\varepsilon \to 0$ yields a system of differential equations that describes the initial postbuckling behavior of the panel:

$$\nabla^4 w_2 + \phi_{2,\xi\xi} + 2\sigma_c w_{2,\xi\xi} - \Lambda_1(\alpha_2 + w_{2,\xi})_{,\xi} - \Lambda_2(\beta_2 + w_{2,\eta})_{,\eta} = 2k\left\{h_1(\eta) + h_2(\eta)\cos\frac{2\pi\xi}{\lambda}\right\}, \tag{36}$$

$$\nabla^4\phi_2 - w_{2,\xi\xi} = 2k\left\{g_1(\eta) + g_2(\eta)\cos\frac{2\pi\xi}{\lambda}\right\}, \tag{37}$$

$$\frac{1-\nu}{2}\nabla^2\alpha_2 + \frac{1+\nu}{2}(\alpha_{2,\xi} + \beta_{2,\eta})_{,\xi} - \Lambda_3(\alpha_2 + w_{2,\xi}) = 0, \tag{38}$$

$$\frac{1-\nu}{2}\nabla^2\beta_2 + \frac{1+\nu}{2}(\alpha_{2,\xi} + \beta_{2,\eta})_{,\eta} - \Lambda_4(\beta_2 + w_{2,\eta}) = 0. \tag{39}$$

The functions appearing on the right-hand sides of equations (36) and (37) are defined in terms of the quantities w_1, ϕ_1 associated with the buckling mode and are given by the relations

$$g_1(\eta) = \frac{1}{2}\left(\frac{\pi}{\lambda}\right)^2\{(w_1'(\eta))^2 + w_1(\eta)\omega_1''(\eta)\}, \tag{40}$$

$$g_2(\eta) = -\frac{1}{2}\left(\frac{\pi}{\lambda}\right)^2\{(w_1'(\eta))^2 - w_1(\eta)w_1''(\eta)\}, \tag{41}$$

$$h_1(\eta) = -\frac{1}{2}\left(\frac{\pi}{\lambda}\right)^2\{\phi_1''(\eta)w_1(\eta) + 2\phi_1'(\eta)w_1'(\eta) + \phi_1(\eta)w_1''(\eta)\}, \tag{42}$$

$$h_2(\eta) = -\frac{1}{2}\left(\frac{\pi}{\lambda}\right)^2 \{\phi_1''(\eta)w_1(\eta) - 2\phi_1'(\eta)w_1'(\eta) + \phi_1(\eta)w_1''(\eta)\}. \tag{43}$$

Observing the structure of the right-hand sides of equations (36–37) it is clear that w_2, ϕ_2, α_2, β_2 may be expressed as

$$\begin{aligned} w_2(\xi,\eta) &= k\left\{\rho(\eta) + \psi(\eta)\cos\frac{2\pi\xi}{\lambda}\right\}, \\ \phi_2(\xi,\eta) &= k\left\{\theta(\eta) + \chi(\eta)\cos\frac{2\pi\xi}{\lambda}\right\}, \\ \alpha_2(\xi,\eta) &= k\left\{\omega(\eta) + \tau(\eta)\sin\frac{2\pi\xi}{\lambda}\right\}, \\ \beta_2(\xi,\eta) &= k\left\{\mu(\eta) + \vartheta(\eta)\cos\frac{2\pi\xi}{\lambda}\right\}. \end{aligned} \tag{44}$$

Eliminating the ξ dependence from equations (36–39) by means of equations (44) one obtains the following set of four independent boundary value problems for the unknown functions appearing in the right-hand sides of equations (44).

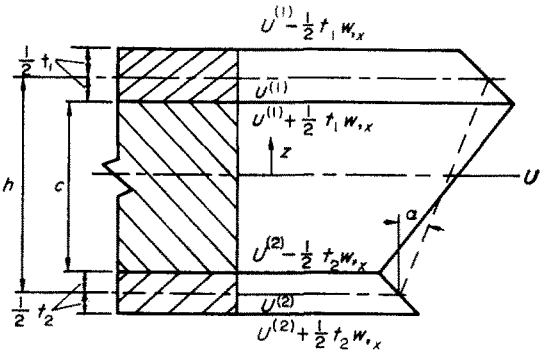

Fig. 2. Cross-section of sandwich panel.

The boundary value problems for the functions $\psi(\eta)$, $\chi(\eta)$, $\tau(\eta)$, $\vartheta(\eta)$; $\rho(\eta)$, $\mu(\eta)$; $\theta(\eta)$; and $\omega(\eta)$ are, respectively:

Problem No. 1

$$\chi^{iv}(\eta) - 2\left(\frac{2\pi}{\lambda}\right)^2 \chi''(\eta) + \left(\frac{2\pi}{\lambda}\right)^4 \chi(\eta) + \left(\frac{2\pi}{\lambda}\right)^2 \psi(\eta) = 2g_2(\eta), \tag{45}$$

$$\psi^{iv}(\eta) - \left\{\Lambda_2 + 2\left(\frac{2\pi}{\lambda}\right)^2\right\}\psi''(\eta) + \left\{\left(\frac{2\pi}{\lambda}\right)^4 - 2\sigma_c\left(\frac{2\pi}{\lambda}\right)^2 + \left(\frac{2\pi}{\lambda}\right)^2 \Lambda_1\right\}\psi(\eta)$$
$$- \left(\frac{2\pi}{\lambda}\right)^2 \chi(\eta) - \Lambda_1\left(\frac{2\pi}{\lambda}\right)\tau(\eta) - \Lambda_2\vartheta'(\eta) = 2h_1(\eta), \tag{46}$$

$$\vartheta''(\eta) - \left\{\Lambda_4 + \frac{1-\nu}{2}\left(\frac{2\pi}{\lambda}\right)^2\right\}\vartheta(\eta) + \frac{1+\nu}{2}\left(\frac{2\pi}{\lambda}\right)\tau'(\eta) - \Lambda_4\psi'(\eta) = 0, \tag{47}$$

$$\frac{1-\nu}{2}\tau''(\eta) - \left\{\Lambda_3 + \left(\frac{2\pi}{\lambda}\right)^2\right\}\tau(\eta) - \frac{1+\nu}{2}\left(\frac{2\pi}{\lambda}\right)\vartheta'(\eta) + \Lambda_3\psi(\eta) = 0, \tag{48}$$

with boundary conditions

$$\psi' = \psi''' = \chi' = \chi''' = \tau' = \vartheta = 0 \quad \text{on} \quad \eta = 0 \tag{49}$$

and

$$\psi = \psi'' = \chi' = \chi'' = \tau = \vartheta' + \nu\left(\frac{2\pi}{\lambda}\right)\tau = 0 \quad \text{on} \quad \eta = \bar{\eta}. \tag{50}$$

Problem No. 2

$$\rho^{iv}(\eta) - \Lambda_2\{\mu'(\eta) + \rho''(\eta)\} = 2h_1(\eta), \tag{51}$$

$$\mu''(\eta) - \Lambda_4\{\mu(\eta) + \rho'(\eta)\} = 0, \tag{52}$$

with

$$\rho' = \rho''' = \mu = 0 \quad \text{on} \quad \eta = 0 \tag{53}$$

and

$$\rho' = \mu' = 0 \quad \text{on} \quad \eta = \bar{\eta}. \tag{54}$$

Problem No. 3

$$\theta^{iv}(\eta) = 2q_1(\eta), \tag{55}$$

with

$$\theta' = \theta''' = 0 \quad \text{on} \quad \eta = 0 \tag{56}$$

$$\theta' = 0 \quad \text{on} \quad \eta = \bar{\eta}. \tag{57}$$

Problem No. 4.

$$\frac{1-\nu}{2}\omega''(\eta) - \Lambda_3\omega(\eta) = 0, \tag{58}$$

$$\omega'(0) = \omega(\bar{\eta}) = 0. \tag{59}$$

The boundary value problems (45–50), (51–54), (55–57), and (58, 59) determine the coefficients appearing in the definitions (44) and hence characterize the initial postbuckling behavior of the composite panel. Equations (58, 59) show that $\omega(\eta) \equiv 0$.

It is shown in[11] that the expansions (35), when they are assumed to be asymptotically valid for $\varepsilon \to 0$, imply a relationship of the form

$$\frac{\sigma}{\sigma_c} = 1 + a\varepsilon + b\varepsilon^2 + 0(\varepsilon^3). \tag{60}$$

It can be shown that the coefficient a in this expansion is identically zero for the composite panel and that

$$b = \frac{2k^2}{\sigma_c}\left\{\frac{\int_0^{\bar{\eta}}[(\phi_1''w_1 - \phi_1 w_1'')\psi + \frac{1}{2}(\phi_1' w_1 - \phi_1 w_1')\psi' - (\phi_1 w_1' + \phi_1' w_1)\rho']\,d\eta}{\int_0^{\bar{\eta}} w_1^2\,d\eta}\right.$$
$$\left. - \frac{1}{4}\frac{\int_0^{\bar{\eta}}[(w_1)^2\chi'' + 4w_1 w_1'\chi' + 4(w_1')^2 - 2(w_1)^2\theta'']\,d\eta}{\int_0^{\bar{\eta}} w_1^2\,d\eta}\right\}. \quad (61)$$

The sign of the initial post-buckling coefficient b determines whether the load increases or decreases immediately after buckling. The significance of the coefficient b is connected with the notions of imperfection-sensitive and imperfection-insensitive structures. It has been shown in[11] that structures containing geometric imperfections (imperfect structures) are imperfection-sensitive, in the sense that the buckling load for the imperfect structure should be expected to be less than the buckling load for the corresponding perfect structure, whenever the load for the perfect structure initially decreases upon bifurcation buckling (see Fig. 3). On the other hand a structure is said to be imperfection-insensitive (in the sense that

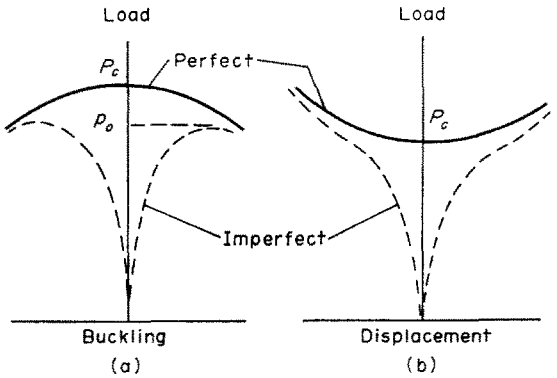

Fig. 3. Generalized load-displacement curves for general structure.

the load-deflection curve for the imperfect structure exhibits a much milder growth of displacement as the load reaches and exceeds the classical buckling load for the perfect structure) whenever the load for the perfect structure increases immediately after bifurcation buckling (see Fig. 3). Accordingly, a structure is said to be imperfection-sensitive or imperfection-insensitive according to whether b is negative or positive. In calculating b it has been assumed that the buckling mode $(w_1, \phi_1, \alpha_1, \beta_1)$ has been normalized so that the maximum value of the physical deflection W_1 is equal to the total thickness of the panel.

Let S denote the initial slope of the load vs end-shortening curve corresponding to the bifurcation path. It is not difficult to show that

$$S = \frac{S_0}{1 + \Delta} \quad (62)$$

where

$$\Delta = \frac{S_0(t^*)^2}{4db\sigma_c}\int_A (w_{1,\xi})^2\,d\xi\,d\eta. \quad (63)$$

Finally, as a measure of the stiffness of the panel immediately after buckling relative to its stiffness prior to buckling we define the stiffness ratio

$$K = \frac{S}{S_0} = \left\{1 + \frac{k^2 \int_A (w_{1,\xi})^2 \, d\xi \, d\eta}{\sigma_c \, b \int_A d\xi \, d\eta}\right\}^{-1}. \tag{64}$$

An expression that is somewhat more convenient to work with is the relative stiffness parameter

$$s = \frac{2}{\pi} \arctan\left(\frac{K}{1-K}\right). \tag{65}$$

Figure 4 indicates how the initial post-buckling coefficient b and the relative stiffness parameter s are to be used to determine the nature of the initial slope of the bifurcation branch. When $b > 0$ and $0 < s < 1$ the initial slope of the buckled path rises so that the buckled structure retains the capacity to carry load in excess of the bifurcation load. This type of

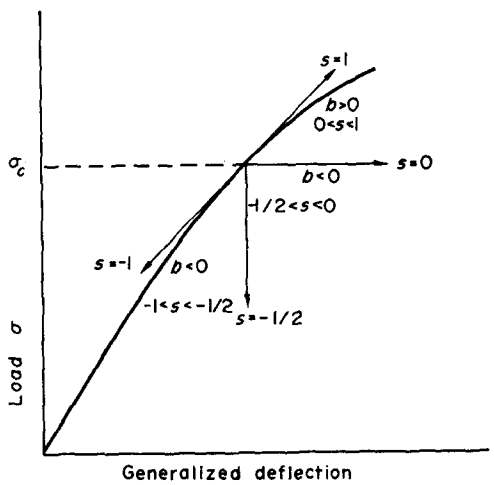

Fig. 4. Graphical description of the initial postbuckling coefficient b and the relative stiffness parameter s.

behavior characterizes the imperfection-insensitive structure. When $b < 0$ and $-0{\cdot}5 < s < 0$ the initial slope of the buckled path is downward to the right and when $b < 0$ and $s < -0{\cdot}5$ the buckled path has a backward sloping tangent. In either case the structure is said to be imperfection-sensitive, i.e. the presence of small geometric imperfections has a significant effect in reducing the load at which the structure will buckle.

NUMERICAL PROCEDURES

Buckling behavior

The linear eigenvalue problem that characterizes the bifurcation load for the composite panel is solved numerically using first order finite difference formulas. Thus, equations

(16–19) along with the boundary and symmetry conditions (20–25) and (28–33), respectively, are replaced by the finite difference analogue

$$\left.\begin{aligned} &A_j Y_{j-1} + B_j Y_j + C_j Y_{j+1} = 0, (j = 1, 2, \ldots, N) \\ &-KY_{-1} + LY_0 + KY_1 = 0, \\ &-GY_{N-1} + HY_N + GY_{N+1} = 0, \end{aligned}\right\} \tag{66}$$

where A_j, B_j, C_j and K, L, G, H are 6×6 matrices and Y_j is a 6×1 column matrix. The lowest eigenvalue for this set of equations can be found conveniently by means of a modified Potters' method[12] that has been suggested by Fulton and Blum[13]. The critical value of the load parameter σ corresponds, therefore, to the minimum value of σ over the range of λ for which the modified buckling determinant

$$M = \frac{(L + KA_0^{-1}B_0)}{|L + KA_0^{-1}B_0|} \cdot \frac{(B_1 + A_1 Q_0)}{|B_1 + A_1 Q_0|} \cdot \frac{(B_2 + A_2 Q_1)}{|B_2 + A_2 Q_1|} \cdots \frac{(B_N + A_N Q_{N-1})}{|B_N + A_N Q_{N-1}|} \cdot DET(D) \tag{67}$$

vanishes. Here

$$DET(D) \equiv DET\{G + (H - GQ_{N-1})Q_N\}. \tag{68}$$

Equations (67) and (68) are arrived at in a natural way through the Gaussian reduction of a tridiagonal set of matrix equations. The quantity $\{G + (H - GQ_{N-1})Q_N\}$ appears as the coefficient of the last unknown column matrix in the reduced triangularized set of matrix equations. Since the system (66) is homogeneous, nontrivial solutions for Y_j exist if and only if $DET(D) = 0$. The lowest value of σ on the set of all wave length ratios λ^* that satisfies $DET(D) = 0$ is the critical load.

The triangularization procedure introduces singularities into the determinant (68) that occur at $DET(D) = 0$. Consequently, in a machine search for the lowest eigenvalue of the system (66) care must be taken not to interpret zeros associated with singularities of equation (68) as zeros associated with eigenvalues. Equation (67) is essentially a quasi-normalized expression of the determinant of the full system (66) and must therefore be a continuous function of σ and λ whose zeros are associated with eigenvalues only.

According to Potters' method the Q_j are given by the recurrence relation

with

$$\left.\begin{aligned} &Q_j = -(B_j + A_j Q_{j-1})^{-1} C_j, (j = 1, 2, \ldots, N) \\ &Q_0 = -(L + KA_0^{-1}B_0)^{-1}(K + KA_0^{-1})C_0. \end{aligned}\right\} \tag{69}$$

To obtain the lowest eigenvalue for the system (66), the load parameter σ was incremented in steps of 1·0 until a sign change in $M(\sigma; \lambda)$ occurred for a fixed value of λ. An interval halving technique was then employed to refine σ to within 1 per cent. This procedure was repeated for 7 values of the wave parameter λ, where the range of λ was selected so as to include the minimum value of σ over all λ.

A seventh order Lagrange interpolating polynomial of the form

$$\sigma(\lambda) = \sum_{k=0}^{7} L_k(\lambda)\sigma_k,$$

with

$$L_k(\lambda) = \prod_{\substack{j=0 \\ k \neq j}}^{7} (\lambda - \lambda_j) / \prod_{\substack{j=0 \\ k \neq j}}^{7} (\sigma_k - \sigma_j), \tag{71}$$

was used to represent the segment of the σ vs λ curve in the range of λ values selected. Differentiation of equation (70) and Newton's method for finding roots of polynomial expressions were used to determine the absolute minimum of σ and the corresponding value of wave parameter λ (see Fig. 5).

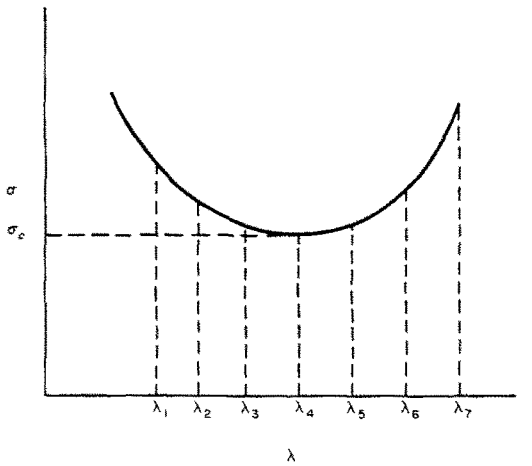

Fig. 5. Plot of dimensionless load parameter σ vs dimensionless wave parameter λ.

Having the critical value of load parameter σ and the corresponding wave parameter λ, the quantities w_1, ϕ_1, α_1, β_1 associated with the buckling mode were calculated by observing that the matrix D appearing in equation (68) is singular for these values. Thus, the rows of D are linearly dependent and, in the present case, a reduced 5×5 system of equations was solved for the vector Y_{N+1}. The vectors $Y_j (j = N, N-1, \ldots, 0)$ are then generated by means of the recurrence relation

$$Y_j = Q_j Y_{j+1}. \tag{72}$$

Vectors Y_j were normalized so that the maximum physical deflection was equal to the total thickness of the composite panel.

Initial post-buckling behavior

The numerical procedures used to obtain solutions for the three linear boundary value problems that characterize the initial post-buckling of the panel are described below.

Boundary value Problem No. 1 (equations 45–50) was solved using the central finite difference analogue

$$\left.\begin{aligned} &A_j Z_{j-1} + B_j Z_j + C_j Z_{j+1} = D_j, (j = 0, 1, \ldots, N) \\ &-KZ_{-1} + LZ_0 + KZ_1 = 0, \\ &-GZ_{N-1} + HZ_N + GZ_{N+1} = 0, \end{aligned}\right\} \tag{73}$$

where A_j, B_j, C_j, K, L, G, H are 6×6 matrices while Z_j and D_j are 6×1 column matrices, Potters' method leads to the recurrence relations

$$Z_j = S_j + Q_j Z_{j+1}, (j = N, N-1, \ldots, 2, 1, 0), \tag{74}$$

$$\left.\begin{aligned} S_j &= (B_j + A_j Q_{j-1})^{-1}(D_j - A_j S_{j-1}), \\ Q_j &= -(B_j + A_j Q_{j-1})^{-1} C_j. \end{aligned}\right\} \tag{75}$$

Starting values for S_j, Q_j, Z_j are obtained from the formulas

$$\left.\begin{aligned} S_0 &= (L + KA_0^{-1}B_0)^{-1}KA_0^{-1}D_0, \\ Q_0 &= -(L + KA_0^{-1}B_0)^{-1}(K + KA_0^{-1}C_0), \\ Z_{N+1} &= \{G + (H - GQ_{N-1})Q_N\}^{-1}\{GS_{N-1} + (GQ_{N-1} - H)S_N\}. \end{aligned}\right\} \tag{76}$$

Calculations for the vectors Z_j are direct; i.e. the process does not involve an iterative procedure.

Boundary value Problem No. 2 (equations 51–54) was solved using a mixed method. Since only first derivatives of $\rho(\eta)$ were required in the computation (the function $\mu(\eta)$ was not needed at all) of the initial postbuckling coefficient b and the relative stiffness parameter s, the function $\mu(\eta)$ was eliminated among the two equations and the result integrated directly to obtain

$$r''(\eta) - (\Lambda_2 + \Lambda_4)r(\eta) = F(\eta), \tag{77}$$

$$r(0) = r(\bar{\eta}) = 0; \tag{78}$$

where

$$r(\eta) = \rho'(\eta) \text{ and}$$

$$F(\eta) = \int_0^{\eta} 2h_1(\lambda)\,d\lambda - \Lambda_4 \int_0^{\eta}\int_0^{\tau}\int_0^{\mu} 2h_1(\lambda)\,d\lambda\,d\mu\,d\tau + \Lambda_4 \frac{\eta}{\bar{\eta}} \int_0^{\bar{\eta}}\int_0^{\tau}\int_0^{\mu} 2h_1(\lambda)\,d\lambda\,d\mu\,d\tau. \tag{79}$$

Values of the function $F(\eta)$ at the mesh points of a finite difference grid were determined numerically using the trapezoidal rule. Having these nodal values for $F(\eta)$, equations (77) and (78) were solved using central finite difference formulas in the same manner as in Problem No. 1. Accordingly, the central difference analogue corresponding to equations (77, 78) is

$$r_{j-1} - [2 + (\Lambda_2 + \Lambda_4)h^2]\, r_j + r_{j+1} = F_j h^2 \tag{80}$$

$$r_0 = r_N = 0, \qquad (J = 1, 2, \ldots, N). \tag{81}$$

Gaussian triangularization leads to the recurrence relationships

$$r_j = Q_j r_{j+1} + S_j, \qquad (j = 1, 2, \ldots, N-1); \tag{82}$$

with

$$\left.\begin{aligned} Q_j &= (k - Q_{j-1})^{-1}, \\ S_j &= -Q_j^{-1}(D_j - S_{j-1}), \end{aligned}\right\} \tag{83}$$

and

$$k = 2 + (\Lambda_2 + \Lambda_3)h^2. \tag{84}$$

The boundary value Problem No. 3 was first integrated directly so as to obtain the required second derivatives

$$\theta''(\eta) = \int_0^{\eta}\int_0^{\mu} 2g_1(\lambda)\,d\lambda\,d\mu - \frac{1}{\bar{\eta}} \int_0^{\bar{\eta}}\int_0^{\tau}\int_0^{\mu} 2g_1(\lambda)\,d\lambda\,d\mu\,d\tau. \tag{85}$$

The function $g_1(\lambda)$ appearing in the integrands of equation (85) is known at the mesh points of the finite difference grid, therefore, the required values of $\theta''(\eta)$ were evaluated using the trapezoidal rule.

The numerical analogues described were programmed on the IBM 670-150 in Fortran IV language using double precision throughout. The finite difference grid spacing was chosen so that the number of interval was always equal to 36.

DISCUSSION OF THE NUMERICAL RESULTS

Figure 6 shows plots of modified buckling parameter $\sigma^* = \sigma/R/t^*$, the initial postbuckling parameter b, and the relative stiffness parameter s, for a wide range of values of the ratio of the transverse shearing modulus of the core material to the Young's modulus of the face-sheets ($g = G_{xz}/E_2$) as functions of the flatness parameter δ/d. The data exhibited in these plots are for the fixed parameters $E_1/E_2 = 1$, $G_{yz}/G_{xz} = 1$, $t_1/t_2 = 1$, and $c/t_2 = 0{\cdot}5$. Torsional resistance of the stiffeners is taken as zero.

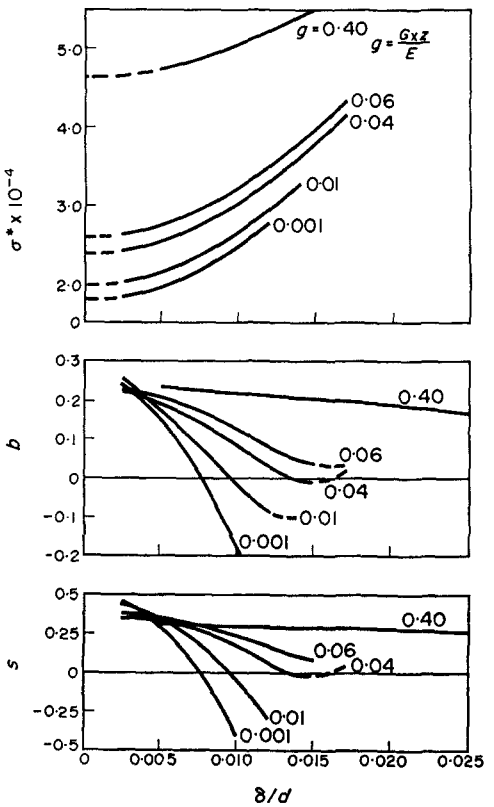

Fig. 6. Effect of transverse shearing resistance on the buckling and initial postbuckling behaviors of sandwich panels ($E_1/E_2 = 1$, $G_{yz}/G_{xz} = 1$, $t_1/t_2 = 1$, $c/t_2 = 0{\cdot}5$, $\gamma_1 = 0$).

First note that for values of g approaching zero, the buckling and initial postbuckling behaviors approach those for a single homogeneous panel as given by Koiter[8]. Also observe that, for small values of δ/d, the panel behaves essentially as a flat plate.

The middle plot of Fig. 6 shows that as the ratio g increases, the range of the flatness parameter δ/d for which the panel remains imperfection-insensitive increases significantly. Moreover, this plot reveals that panels for which g is realistic are unlikely to be imperfection-sensitive.

Finally, the bottom plot of Fig. 6 indicates that, for the range of δ/d considered, panels for which g is realistic are not likely to have backward sloping load-deflection curves. Indeed, it is quite likely that the postbuckling branch will rise and hence possess the characteristic of a flat plate.

The curves exhibited in Fig. 6 generally extend to the limit of applicability of the theory with regard to the flatness parameter δ/d. However, while no detailed investigation has been made to establish quantitatively how the various material and geometric parameters that characterize the sandwich panel effect the range of applicability of the theory it can be concluded that each parameter considered as a family parameter in this study increases this range.

Figure 7 shows the effect that different relative face-sheet thicknesses have on the buckling and initial postbuckling behavior of the sandwich panel. The plots are obtained for fixed values of $G_{xz}/E_2 = 0{\cdot}04$, $E_1/E_2 = 1$, $G_{yz}/G_{xz} = 1$, $c/t_2 = 1$ and zero torsional resistance of

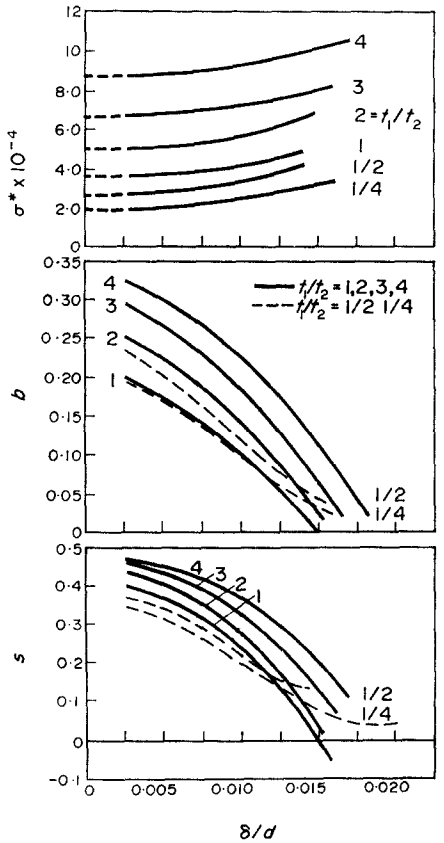

Fig. 7. Effect of different face-sheet thicknesses on the buckling and initial postbuckling behaviors of sandwich panels ($G_{xz}/E_2 = 0{\cdot}04$, $G_{yz}/G_{xz} = 1$, $E_1/E_2 = 1$, $c/t_2 = 1$, $\gamma_1 = 0$).

the stiffeners. Again, one observes what one expects relative to the buckling behavior. Note that the range of imperfection–insensitivity increases as the ratio of the outer face-sheet thickness to the inner face-sheet thickness increases. This observation also seems to be valid for ratios $t_1/t_2 < 1$, however, the flattening effect observed for these curves for higher values of δ/d may reflect the nearing of the end of the range of validity for the theory.

Figure 8 shows the effect of different values of h/t_2 on the buckling and initial post-buckling behavior when $G_{xz}/E_2 = 0{\cdot}04$, $E_1/E_2 = 1$, $G_{yz}/G_{xz} = 1$, $t_1/t_2 = 1$ and the torsional resistance of the stiffeners is zero.

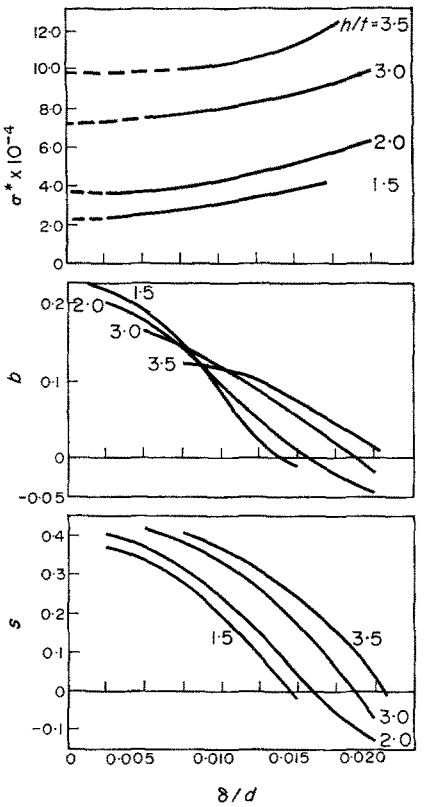

Fig. 8. Effect of different core thicknesses on the buckling and initial postbuckling behaviors of sandwich panels ($G_{xz}/E_2 = 0{\cdot}04$, $G_{yz}/G_{xz} = 1$, $E_1/E_2 = 1$, $t_1/t_2 = 1$, $\gamma_1 = 0$).

Again the range of δ/d for which the panel remains imperfection-insensitive is increased with increasing values of h/t_2. It is interesting to note that for small values of δ/d (nearly flat plates) the initial postbuckling coefficient decreases significantly for increasing values of h/t_2. This may be an indication that an imperfection–sensitive condition can arise for a flat sandwich plate under certain conditions—notably when the ratio g is small and the ratio of the distance between the middle surfaces of the face-sheets and the face-sheet thickness is large.

Figure 9 shows the effect of torsional resistance of the edge stiffeners on the buckling and initial postbuckling behaviors of the sandwich panel for various values of the ratio $g = G_{xz}/E_2$ when $E_1/E_2 = 1$, $G_{yz}/G_{xz} = 1$, $t_1/t_2 = 1$, $c/t_2 = 0{\cdot}5$, and $\delta/d = 0{\cdot}008$.

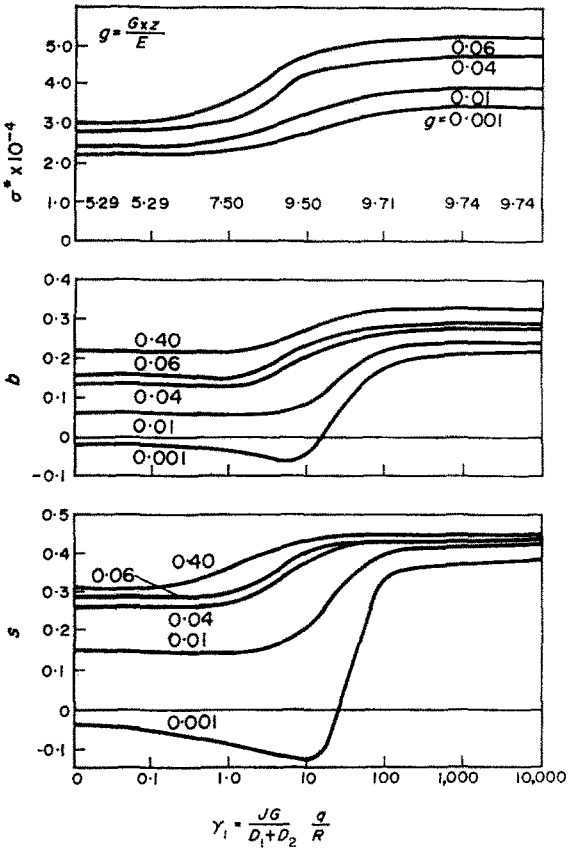

Fig. 9. Effect of torsional resistance on the buckling and initial postbuckling behaviors of Sandwich panels with $G_{xz}/G_{yz} = 1$, $E_1/E_2 = 1$, $t_1/t_2 = 1$, $c/t_2 = 0{\cdot}5$, $\delta/d = 0{\cdot}008$.

The numbers appearing in the upper plot of Fig. 9 correspond to values of σ^* for $g = 0{\cdot}40$. These values were not plotted so that the remaining curves could be situated on the same page.

The buckling behavior indicates a substantial increase in the buckling resistance of sandwich panels as the support condition changes from an essentially simple-support for small values of torsional resistance parameter γ_1 to a clamped support for large values of γ_1. Clearly, the presence of significant torsional resistance in the longitudinal stiffeners tends to reduce the degree of imperfection-sensitiveness and has the greater effect for smaller values of g.

Figure 10 shows the effect of torsional resistance of the longitudinal stiffeners on the buckling and initial postbuckling behaviors of the sandwich panel for various values of h/t_2 when $G_{xz}/E_2 = 0{\cdot}04$, $E_1/E_2 = 1$, $G_{yz}/G_{xz} = 1$, $t_1/t_2 = 1$, and $\delta/d = 0{\cdot}008$.

The buckling behavior appears as one expects, i.e. the buckling resistance of the sandwich panel increases from the values characterizing the simple-support condition ($\gamma_1 = 0$) to those associated with the clamped support (γ_1 large).

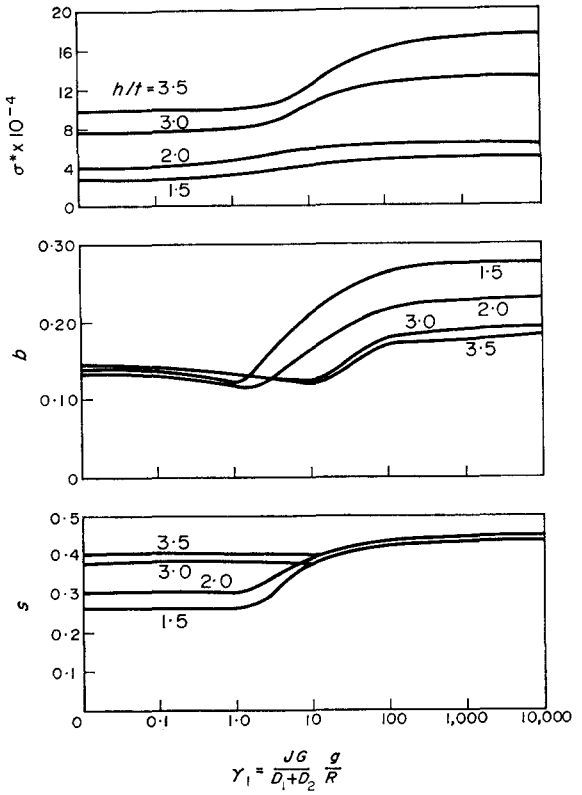

Fig. 10. Effect of torsional resistance on the buckling and initial post-buckling behaviors of sandwich panels with h/t_2 as a family parameter ($G_{xz}/E_1 = 0{\cdot}04$, $G_{yz}/G_{xz} = 1$, $E_1/E_2 = 1$, $t_1/t_2 = 1$, $\delta/d = 0{\cdot}008$).

It is interesting to note that the initial post-buckling coefficient b, for large values of torsional resistance of the stiffeners, decreases sharply as h/t_2 is increased. However, b appears to be approaching an asymptotic value that lies in the imperfection–insensitive region.

REFERENCES

1. R. E. Fulton, Nonlinear equations for a shallow unsymmetrical sandwich shell of double curvature, *Proc. 7th Midwestern Mech. Conf.*, p. 365. Michigan State University (1961).
2. N. Akkas and N. R. Bauld, Jr., Buckling and initial post-buckling behavior of clamped shallow spherical sandwich shells, *Int. J. Solids Struct.* 7, 1237 (1971).
3. N. S. Khot, On the effects of fiber orientation and nonhomogeneity on buckling and initial post-buckling equilibrium behavior of fiber-reinforced cylindrical shells under uniform axial compression. *Tech. Rep.* AFFDL-TR-68-19, Air Force Flight Dynamics Laboratory, Air Force Systems Command, Wright-Patterson Air Force Base, Ohio (May 1968).
4. N. S. Khot, On the influence of initial geometric imperfections on the buckling and initial post-buckling behavior of fiber-reinforced cylindrical shells under uniform axial compression. *Tech. Rep.* AFFDL-TR-68-136, Air Force Flight Dynamics Laboratory, Air Force Systems Command, Wright-Patterson Air Force Base, Ohio (October 1968).
5. N. S. Khot and V. E. Venkayya, Effect of fiber orientation on initial post-buckling behavior and imperfection sensitivity of composite cylindrical shells. *Tech. Rep.* AFFDL-TR-70-125, Air Force Flight Dynamics Laboratory, Air Force Systems Command, Wright-Patterson Air Force Base, Ohio (Dec. 1970).

6. J. W. Hutchinson and W. T. Koiter, Postbuckling behavior, *AMR*, **23**, 1353 (1970).
7. G. G. Pope, The buckling behavior in axial compression of slightly-curved panels, including the effect of shear deformability, *Int. J. Solids Struct.* **4**, 323 (1968).
8. W. T. Koiter, Buckling and postbuckling behavior of a cylindrical panel under axial compression, *Repr.* S.476 (1956). National Aeronautical Research Institute, Amsterdam.
9. W. B. Stephens, Imperfection sensitivity of stringer reinforced cylindrical panels under internal pressure, *AIAA J.* **9**, 1713 (1971).
10. W. T. Koiter, Over de Stabiliteit van Het Elastisch Evenwicht ("On the Stability of Elastic Equilibrium"), Thesis, Delft, H. J. Paris, Amsterdam, 1945. English translation issued as NASA TT-F-10, 833 (1967).
11. B. Budiansky, Dynamic buckling of elastic structures; criteria and estimates, *Proc. Int. Conf. Dynamic Stability of Structures*, pp. 83–106. Pergamon Press (1966).
12. M. L. Potters, A. Matrix method for the solution of a second order difference equation in two variables, *Rep.* MR19, Mathematich Centrum, Amsterdam, Holland (1955).
13. R. E. Blum and R. E. Fulton, A modified Potters' method for solving eigenvalue problems involving tridiagonal matrices, *AIAA J.* **4**, 2231 (1966).

Резюме — В настоящей работе рассматривают численные результаты влияния нескольких безмерных параметров на коробление и на исходное, следующее за короблением, поведение неглубоких многослойных панелей, подвергнутых осевому сжатию. По результатам видно, что эти эффекты возникают вследствие сопротивления поперечному сдвиговому деформированию материала сердечника, вследствие больших поперечников грани-листов и сердечника. Добавочное влияние на коробление и на следующее за короблением поведение, оказывает сопротивление кручению продольных элементов жесткости кромок.

Из результатов следует, что коэффициент плоскосности, δ/d, при которых неглубокие многослойные панели остаются нечувствительными к искажению повышается с повышением сопротивления поперечному сдвиговому деформированию материала сердечника и при бóльшей толщине сердечника. Результаты также указывают, что коэффициент, δ/d, самый малый, когда толщины грани-листа одинаковые. И наконец, как в случае однородных панелей, сопротивление кручению продольных ребер жесткости кромок делает неглубокие многослойные панели менее чувствительными к искажению.